Results in Physics 8 (2018) 903–907

Contents lists available at ScienceDirect

Results in Physics

journal homepage: www.journals.elsevier.com/results-in-physics

Deposition of Cu-doped PbS thin films with low resistivity using DC sputtering

Hariyadi Soetedjo [a,b,*], Bambang Siswanto [c], Ihwanul Aziz [c], Sudjatmoko [c]

[a] Study Program of Physics (Metrology-Electronics Material-Instrumentations), FMIPA, University of Ahmad Dahlan, Jalan Prof. Dr. Soepomo, S.H., Yogyakarta 55164, Indonesia
[b] CIRNOV, University of Ahmad Dahlan, Jalan Cendana No 9A, Semaki, Yogyakarta 55166, Indonesia
[c] PSTA – BATAN, Jalan Babarsari, Kotak Pos 6010, Yogyakarta 55281, Indonesia

ARTICLE INFO

Article history:
Received 20 October 2017
Received in revised form 30 December 2017
Accepted 6 January 2018
Available online 11 January 2018

Keywords:
Thin films
Lead sulfide
Sputtering
Resistivity
Semiconductor
Infrared

ABSTRACT

Investigation of the electrical resistivity of Cu-doped PbS thin films has been carried out. The films were prepared using a DC sputtering technique. The doping was achieved by introducing the Cu dopant plate material directly on the surface of the PbS sputtering target plate. SEM-EDX data shows the Cu concentration in the PbS film to be proportional to the Cu plate diameter. The XRD pattern indicates the film is in crystalline cubic form. The Hall effect measurement shows that Cu doping yields an increase in the carrier concentration to 3.55×10^{19} cm^{-3} and a significant decrease in electrical resistivity. The lowest resistivity obtained was 0.13 Ωcm for a Cu concentration of 18.5%. Preferential orientation of (1 1 1) and (2 0 0) occurs during deposition.

Introduction

Lead sulfide (PbS) is a well-known semiconductor material with interesting properties. It has a direct and narrow bandgap of 0.41 eV at room temperature [1]. PbS has high absorbance in the UV–Vis spectral range and high transmittance in the infrared spectral region of 1–3 μm [2], allowing its use in infrared detectors. This material also has applications in other opto-electrical devices such as solar cells. The electrical properties of PbS thin films can be tailored by introducing dopants into the material and depositing the film on various substrates, such as glass [3,4], silicon [5], and glass/silicon [6] by techniques such as chemical bath deposition (CBD). Akmedov [7] prepared PbS films using a simple chemical deposition.

The dopants Zn [8] and Sr [9] have been incorporated into PbS using CBD, and Ba using the successive ionic layer adsorption and reaction (SILAR) technique [10]. Cheraghizade et al. [11] prepared a Zn-doped PbS thin film using chemical vapor deposition (CVD) for photovoltaic devices. PbS nanocrystal-doped SiO_2 films were prepared using sputtering [12] and the material structure and properties were investigated. Also, Bi-doped PbS quantum dots were prepared for photovoltaic devices [13].

Cu-doped PbS thin films have also been studied by many researchers for various applications. Preparations of Cu-doped PbS thin films by CBD have been reported [14–17]. Zheng et al. [14] prepared Cu-doped PbS thin films to study the low resistivity of the material. The result obtained has been encouraged our work to prepare more robust thin films with low resistivity using a DC sputtering technique. This was done by introducing Cu plate as a dopant material. Beside, a novel method introduced for doping process using a dopant plate putting directly on the surface of the material target. By using this technique other dopant materials such of Fe could also be introduced with a simple way and practical. By comparing the work done using sputtering technique to the other technique of CBD, the sputtering technique produces more robust PbS film deposition and relatively faster in deposition time. In the present study, we improve the investigation for the structural and morphological properties of PbS and Cu-doped PbS thin films using SEM-EDX and investigate the electrical properties using a Hall effect technique. The interesting properties observed from the material is its lower resistivity film compare the other works

* Corresponding author at: Study Program of Physics (Metrology-Electronics Material-Instrumentations), FMIPA, University of Ahmad Dahlan, Jalan Prof. Dr. Soepomo, S.H., Yogyakarta 55164, Indonesia.
E-mail address: superadmin@cirnov.uad.ac.id (H. Soetedjo).

https://doi.org/10.1016/j.rinp.2018.01.020
2211-3797/

published previously that will be reported. Also, the detail explanation of the doping effect introduced to the material.

Experimental

Synthesis

PbS thin film deposition was prepared using a DC sputtering technique. The PbS target plate was 99.9% purity (QS Rare Element) with 2.0 in. diameter and 0.12 in. thickness. The dopant plate of Cu (99.9% purity, Goodfellow) with 0.5 mm thickness was put onto the PbS target plate at the center position. Various Cu concentrations (wt%) were incorporated into the PbS thin films. Samples 0, 1, 2, 3, 4 and 5 denote the samples with Cu plate diamater and concentrations as tabulated in Table 1. During the sputtering process, the vacuum pressure was maintained at 2.0×10^{-2} Torr, the distance between target and substrate was 3 cm. The power of sputtering process was supplied for 20 Watt. A glass microscope slide with deposition area of 1.0×2.5 cm^2 was used as the substrate. All samples were deposited for 30 min at the same condition. The substrate was placed at the anode (top position), while the target material was at the cathode (bottom position) as shown in Fig. 1. This orientation was adjusted to minimize contaminant deposition during the sputtering process. The distance between the anode and cathode was adjusted to 3 cm.

Table 1
Some parameters of thin film deposition.

Sample no	Plate diamater (mm)	Cu concentration (wt%)
0	–	0.0
1	5.0	2.8
2	7.5	4.0
3	10.0	10.5
4	15.0	18.9
5	20.0	31.2

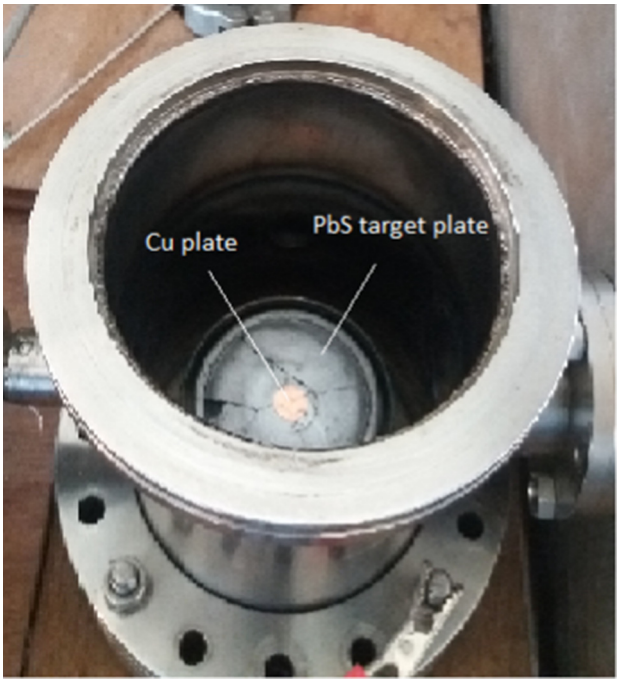

Fig. 1. The photograph of PbS target and Cu dopant plate in the vacuum chamber.

Methods

Material structures of the film were characterized using X-ray diffraction (XRD) with CuK_α radiation source ($\lambda = 1.54$ Å) and the morphology of film was characterized using SEM-EDX. The Hall effect measurement was also carried out in order to investigate electrical properties of the films, such of carrier concentration, mobility, and resistivity.

Results and discussion

The samples were measured using SEM-EDX to study the morphological surface and to find the elemental composition (Pb, S, Cu) of the films (Figs. 2a and 2b). As we can see in Fig. 2a from the SEM measurement, the undoped PbS deposition has homogeneous surface morphology and smooth with very good grain boundaries. The average grain size is calculated and found to be 35 nm. The results indicate successful doping of PbS by Cu using the sputtering method described. The increase in diameter of the dopant plate results in an increase in concentration of dopant in the PbS thin film. This thin film preparation method is considerably new for DC sputtering, particularly for Cu as a dopant material. Common method used was done by mixing the target material with the doping material prior to the deposition using a special method that needs additional work leads to time consuming, impractical and costly.

XRD patterns of the Cu-doped PbS thin films are shown in Fig. 3. The calculated diffraction plane (Miller index) refers to the index printed on the axis of the database (JCPDS, Card No 05-0592). The Bragg peaks obtained were in good agreement with the database, indicating cubic crystalline structure. The peak intensities observed from the diffraction planes (1 1 1) and (2 0 0) change with the elemental composition of each film. For Cu concentrations of 10.5% and 18.9%, the peaks observed at (1 1 1) and (2 0 0) are relatively sharp, indicating high crystallinity. Thus, these Cu concentrations are preferential for film deposition. At the doping concentration of 31.2%, the Bragg peaks become broadened, indicating

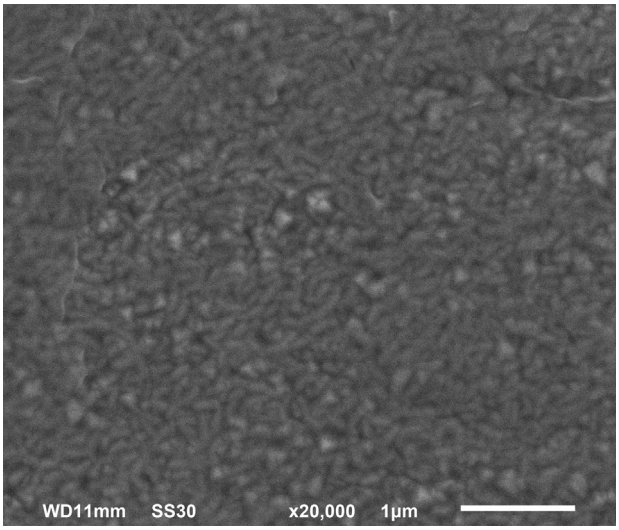

Fig. 2a. Morphological image obtained from SEM for PbS thin film sample.

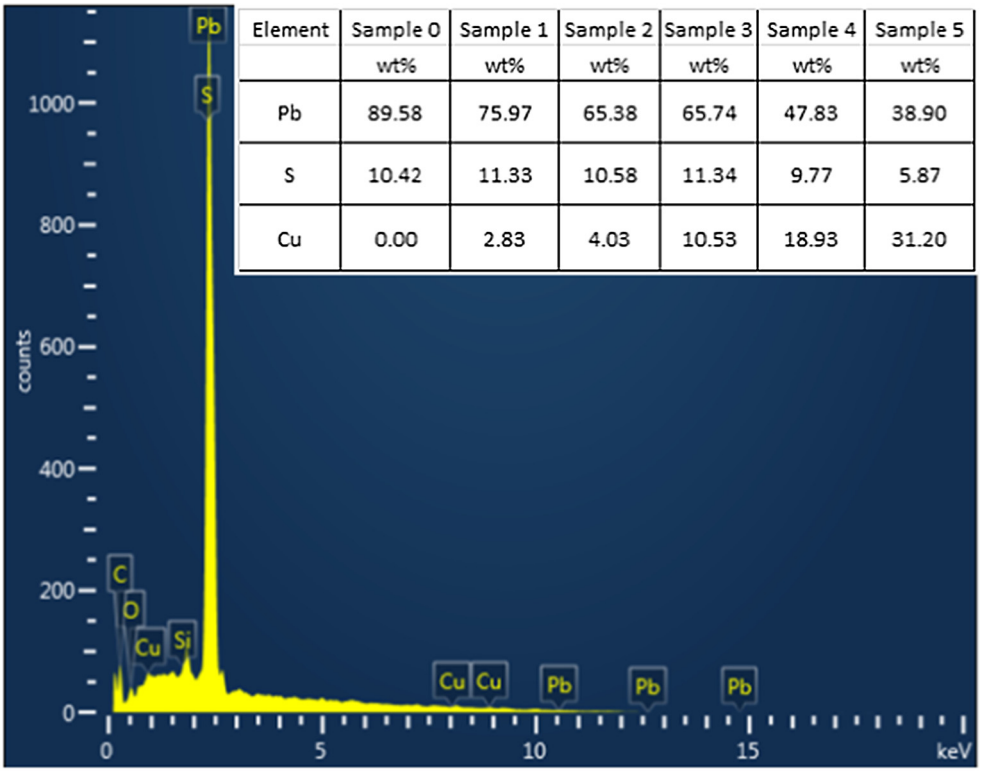

Element	Sample 0	Sample 1	Sample 2	Sample 3	Sample 4	Sample 5
	wt%	wt%	wt%	wt%	wt%	wt%
Pb	89.58	75.97	65.38	65.74	47.83	38.90
S	10.42	11.33	10.58	11.34	9.77	5.87
Cu	0.00	2.83	4.03	10.53	18.93	31.20

Fig. 2b. Representative EDX data (Sample 1) and elemental compositions (inset table) of each Cu-doped PbS thin film sample.

that the crystal structure contained defects or became less crystalline.

The texture coefficient (*TC*) of preferential direction was deduced from the observed Bragg peaks (Fig. 4). This coefficient indicates the degree of crystallinity formed during the deposition of the thin film, and is calculated using the following equation [15]:

$$TC = \frac{I(hkl)/Io(hkl)}{\frac{1}{N}\sum_N \left(\frac{I(hkl)}{Io(hkl)}\right)} \quad (1)$$

where, $I(hkl)$ is the measured intensity of (hkl) plane of the sample, $Io\ (hkl)$ is the standard intensity of (hkl) plane based on the powder diffraction file (JCPDS) card, and N is the number of diffraction peaks considered in the analysis. From the calculation, the *TC* at the diffraction plane of (1 1 1) and (2 0 0) appears more stable with an increase of Cu concentration from 10.5 to 18.9%. Higher Cu concentrations appear to reduce crystallinity of the thin films, as can be seen from the XRD pattern. An interesting phenomenon observed is that with the relatively stable growth (Cu doping concentration of 18.9%), a minimum resistivity is achieved.

The carrier concentration in the PbS films increases to a maximum as the Cu dopant concentration increases from 2.8 to 18.9% (solid data points in Fig. 5a). Then, for 31.2% Cu dopant, the carrier concentration decreases. This trend was also observed by Zheng et al. [14] and Touati et al. [15]. The increase in carrier concentration occurs because the substitution of Cu ions for Pb ions induces more vacancies [14]. This increase is attributed to the mid-gap state created by Cu doping that traps and screens electrons, as explained by Huang et al. [18]. With further doping, excess Cu atoms can not occupy lattice sites. They form neutral defects that become ineffective as carriers, leading to a decrease in carrier concentration. As can be seen in Fig. 5a, the maximum value of carrier concentration is 3.55×10^{19} cm^{-3}, achieved at a Cu concentration of 18.9%.

The increase in Cu doping (up to 31.2%) yields fluctuations of carrier mobility ranging from around 148 cm^2/V·s down to 16 cm^2/V·s (open data points in Fig. 5b), with an overall decreasing trend. Similarly, a decrease in carrier mobility from around 110 cm^2/V·s down to 6 cm^2/V·s was observed by Zheng et al. [14] for Cu concentrations increasing up to 8%. Regarding carrier mobility, the highest value is observed in the undoped PbS film. The increased mobility is assumed to be due to the Coulombic interactions among the carriers that form electron traps and screens, as mentioned before. The carriers introduce a longer, mean-free time of collision that increases mobility. Meanwhile, the decreased mobility at higher Cu concentration is due to the Cu ions forming ineffective neutral defects. This phenomenon can be attributed to scattering and defects caused by excess carriers [18]. The defects in the crystal structure can be observed as broadened peaks in the XRD patterns (Fig. 3).

The increase in Cu dopant concentration up to 18.9% in the PbS films is followed by a decrease in resistivity. A further increase in Cu dopant concentration yields an increase in resistivity. These effects show that introducing Cu doping to PbS films changes the electrical properties of the material significantly. A Cu concentration of 18.9% achieves a minimum resistivity value of 0.13 Ωcm (Fig. 5b). A comparison of resistivity values from previous works is shown in Table 2. In this current work, we report a relatively low resistivity, achieved by using a DC sputtering technique for Cu-doped PbS thin film formation. Beside, the simple method of doping was introduced in the sputtering deposition technique.

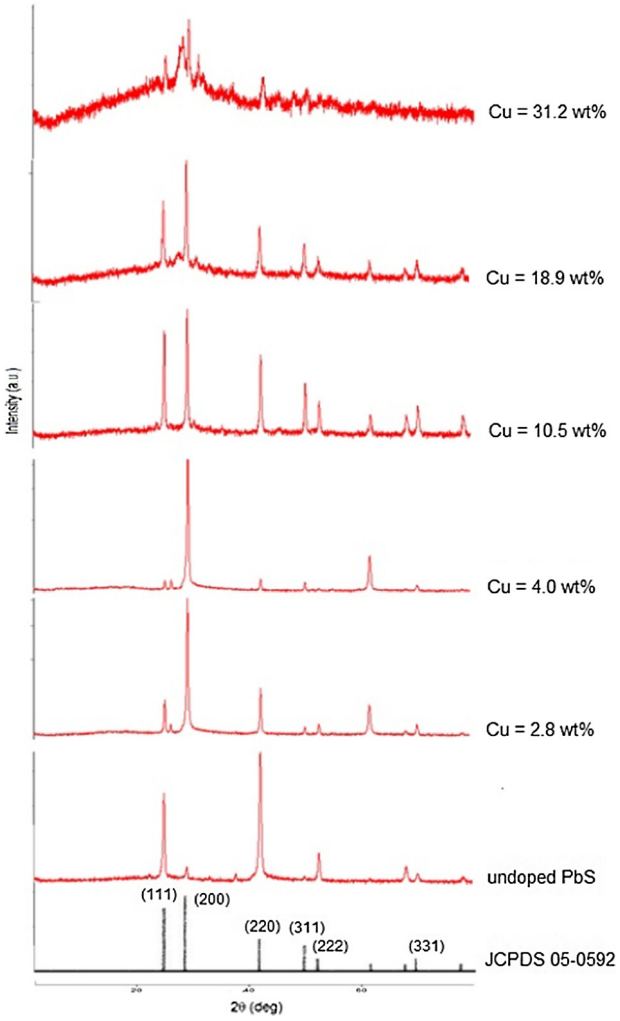

Fig. 3. XRD patterns obtained for each Cu-doped PbS thin film sample. The calculated diffraction plane (Miller index) refers to the index printed on the axis of the database.

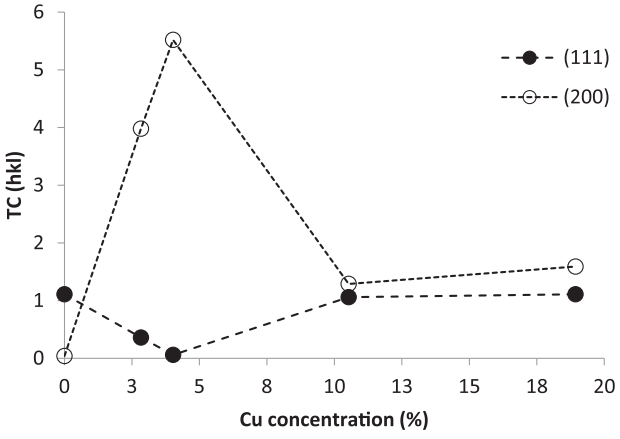

Fig. 4. *TC* for (1 1 1) and (2 0 0) directions in Cu-doped PbS thin films.

Conclusion

Cu-doped PbS thin films have been successfully prepared using a DC sputtering technique. The film deposition has good crystallinity, as shown by the XRD measurement. From Hall measurements, it was shown that the carrier concentration has a maximum value of 3.55×10^{19} cm^{-3} at 18.9% dopant concentration. The increase of Cu concentration is followed by an increase of carrier concentration until the maximum value, after which it decreases. In comparison to values in the literature, a relatively lowest resistivity of 0.13 Ωcm was obtained with an 18.9% Cu concentration. The use of Cu as a dopant is an effective method of improving the electrical resistivity of PbS thin films for device applications.

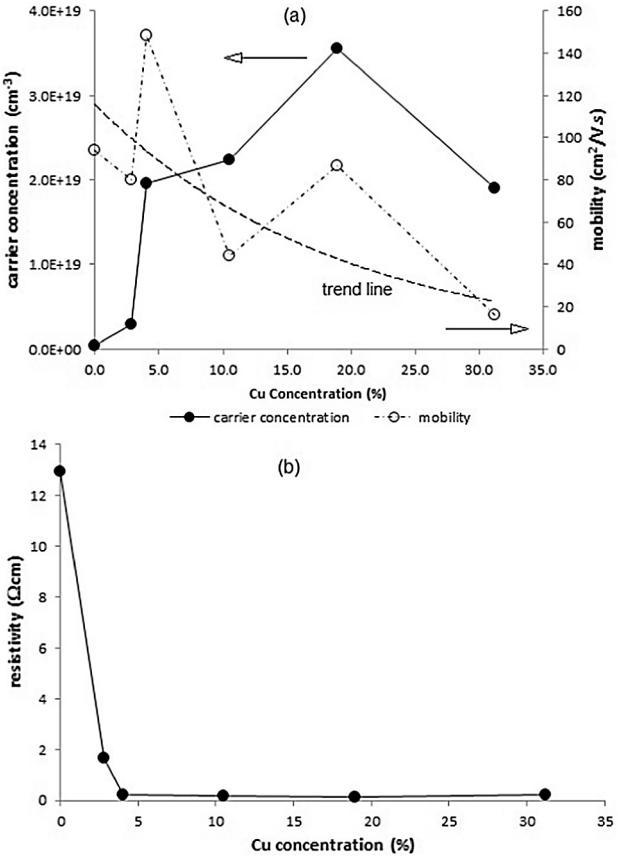

Fig. 5. Effect of Cu doping concentration in PbS films on (a) carrier concentration and mobility, and (b) resistivity.

Table 2
Resistivity values for Cu-doped PbS thin films obtained from the literature.

Deposition technique	Resistivity (Ω·cm)	Reference
DC sputtering	0.13	current work
CBD	0.15	Zheng [14]
CBD	0.16	Touati [15]
CBD	4.1	Pérez-García [16]

References

[1] Barote MA, Yadav AA, Chavan TV, Masudar EU. Digest J Nanomat Biostruct 2011;6(3):979–90.
[2] Choudhary N, Sarma BK. Bull Mater Sci 2009;32(1):43–7.
[3] García-Valenzuela JA, Baez-Gaxiola MR, Sotelo-Lerma M. Thin Sol Films 2013;534:126–31.
[4] Thirumavalava S, Mani K, Suresh S. J Ovonic Res 2015;11(3):123–30.
[5] Tohidi T, Jamshidi-Ghaleh K. Phil Mag 2014;94(29):3368–81.
[6] Nasir EM, Abbas MM. Chalcogen Lett 2016;13(6):271–9.

[7] Akhmedov OR, Guseinaliyev MG, Abdullaev NA, Abdullaev NM, Babaev SS, Kasumov NA. Semicond 2016;50(1):50–3.
[8] Singh LR, Singh SB, Rahman A. Chalcogen Lett 2013;10(5):167–72.
[9] Yücel E, Yücel Y. Ceramics Int 2017;43:407–13.
[10] Gülen Y. Acta Phys Polonica A 2014;126(3):763–7.
[11] Cheraghizade M, Jamali-Sheini F, Yousefi R. Appl Phys A 2017;123:390.
[12] Reiche R, Thielsch R, Oswald S, Wetzig K. J Electr Spectros Related Phenom 1999;104:161–71.
[13] Stravinadis A, Rath AK, de Arquer FPG, Diedenhofen SL, Magén C, Martinez L, et al. Nature Com. 2013;1–7.
[14] Zheng X, Gao F, Ji F, Wu H, Zhang J, Hu X, Xiang Y. Mater Lett 2016;167:128–30.
[15] Touati B, Gassoumi A, Dobryden I, Natile MM, Vomiero A, Turki NK. Superlatt Microstruct 2016;97:519–28.
[16] Pérez-García CE, Ramírez-Bon R, Vorobiev YV. Chalcogen Lett 2015;12 (11):579–88.
[17] Palomino-Merino R, Palomino-Moreno O, Flores-Garcia JC, Hernandez-Tecorralco J, Martinez-Juarez J, Moran-Torres A, et al. J Nanosci Nanotechn 2014;14(7):5408–14.
[18] Huang Z, Zou X, Zhou H. Mat Lett 2013;95:139–41.